applied sciences

MDPI

Article

High-Performance Color-Converted Full-Color Micro-LED Arrays

Won Hee Kim [1], Young Jae Jang [1], Ja-Yeon Kim [2], Myungsoo Han [3], MinJae Kang [3], Kiyong Yang [3], Jae-Hyun Ryou [4] and Min-Ki Kwon [1,*]

1 Department of Photonic Engineering, Chosun University, Gwangju 501-759, Korea; love_misan@naver.com (W.H.K.); zqwasd2359@naver.com (Y.J.J.)
2 Korea Photonics Technology Institute (KOPTI), Gwangju 500-460, Korea; jykim@kopti.re.kr
3 LG Display, E2 Block LG Science park, 30, Magokjungang 10-ro, Gangseo-gu, Seoul 07796, Korea; mshan@lgdisplay.com (M.H.); sim40@lgdisplay.com (M.K.); truecourage@lgdisplay.com (K.Y.)
4 Department of Mechanical Engineering, University of Houston, Houston, TX 77204-2004, USA; jryou@Central.UH.EDU
* Correspondence: mkkwon@chosun.ac.kr; Tel.: +82-62-230-7549

Received: 4 February 2020; Accepted: 11 March 2020; Published: 20 March 2020

Abstract: Color-converted micro-LED displays consisting of mono-blue-colored micro LED arrays and color-conversion materials have been used to achieve full color while reliving the transfer and epitaxial growth of three different-colored micro LEDs. An efficient technique is suggested to deposit the color-conversion layers on the blue micro LEDs by using a mixture of photo-curable acrylic and nano-organic color-conversion materials through the conventional lithography technique. This study attempts to provide a solution to fabricate full-color micro-LED displays.

Keywords: micro LED; full color; GaN; light-emitting diode; color-conversion

1. Introduction

The micro-LED display is a technology that has expanded rapidly in recent years because of its outstanding features such as low power consumption, quick response, long lifetime, and wide color gamut [1–4]. However, the fabrication of full-color micro-LED arrays is still under the process of channeling. The most commonly used routes to fabricate these devices involve epitaxial growth of red, green, and blue (RGB) active materials on different substrates followed by chip fabrication, wafer dicing, and pick-and-place robotic manipulation into individually packaged components for interconnection by bulk wire bonding. However, dicing becomes more difficult as the chip size decreases beyond 100 μm × 100 μm, and integrating them on the same thin-film transistor-based glass substrates through mass transfer, which requires precise alignment for each pixel, becomes a challenge [5–7]. Moreover, the light-emission efficiencies and degradation rates of RGB micro LEDs are different; as a result, a complicated driving circuit may be needed to maintain the color-rendering index during operation.

A simpler method to achieve full color without mass transfer of individual R, G, B chips is to utilize the color filters to achieve RGB subpixels while generating white light by deposition of a yellow color converter on blue micro-LEDs [5,6]. In this device configuration, the color downconversion layer does not need to be pixilated; thereby it becomes more feasible for manufacturing. However, the color filters would absorb two-thirds of the outgoing light. In addition, color crosstalk would occur, owing to scattering of the color-conversion layer.

Another approach to avoid the mass-transfer process is the fabrication of full-color micro LEDs based on blue or UV micro LEDs and color-conversion materials of blues, greens, and reds. For color-conversion materials, nanophosphors and quantum dots (QDs) can be used [8–11]. For example,

Han et al. [9] deposited RGB QDs on top of a UV LED array using the aerosol jet printing method to form individual subpixels. This configuration is advantageous in that it does not require a color filter and offers a possibility of achieving high efficiency and a wide color gamut. However, a thick layer of QDs with high optical density is required for high color downconversion efficiency. In addition, longer processing times and special equipment are required.

So, there is a need for a method that can deposit a large amount of color-conversion materials on blue pixels in a single process with precise alignment for each pixel. Photolithography is a useful method to achieve this purpose. However, there is no report on the fabrication of a micro-sized color-conversion layer based on photolithography. In this paper, we propose an efficient technique to fabricate full-color micro-LED pixels using the mixture of photocurable acrylic and nano-organic color-conversion materials by conventional lithography technique. We can significantly control the position, size, and thickness of the color-conversion layers to fabricate full-color micro LEDs. This study attempts to provide a solution for fabricating full-color micro-LED displays.

2. Experimental Section

Figure 1 illustrates the device structure of color-converted full-color micro LEDs based on mono-blue-color micro LEDs. It consists of bottom blue micro-LED arrays and a layer of two color (green and red)-conversion materials. The total array size is 100 × 100 pixels in a chip area of 10 × 10 mm^2. The chip size of the blue micro LED is 60 × 100 μm^2 and the pitch length of each pixel is 300 μm. A GaN-based LED structure (operating at a dominant emission peak of 450 nm) was grown on a sapphire substrate using metal–organic chemical vapor deposition. The LEDs consisted of a 2 μm Si-doped n-GaN layer, a molecular quantum well (MQW) active layer consisting of five periods of undoped InGaN wells and undoped GaN barriers, and a 0.15 μm Mg-doped p-GaN layer. To fabricate the LEDs, the p-GaN layer was etched using an inductively-coupled plasma (ICP) that utilized Cl_2 and BCl_3 source gases until the n-GaN layer was exposed for n-type contact. Further, the LEDs were fabricated using a 200 nm-thick indium tin oxide (ITO) layer as a transparent current spreading layer. Layers of Cr and Au with thicknesses of 30 nm and 100 nm, respectively, were deposited by e-beam evaporation as the n- and p-pad electrodes, respectively. The SiO_2 passivation layer was coated on the wafer for array electrode fabrication. Further, the SiO_2 layer on the n- and p-pad was selectively etched by buffer oxide etchant (BOE) until the n- and p-pad electrodes were exposed to the array electrode. Layers of Cr and Au with thicknesses of 100 nm and 500 nm, respectively, were deposited by e-beam evaporation as the n- and p-array electrodes, respectively. To avoid the color-crosstalk effect, black matrix was deposited between the blue LEDs by using simple lithography techniques.

To fabricate conformal color-conversion layers, green, and red perylene bisimide were mixed with organic insulator material, a solution of acrylic resin, and a photoactive compound (PAC) with a positive tone of diazonaphthoquinone (DNQ). Perylene bisimide is known to have strong absorption in the visible region and high fluorescence quantum yields (QY) in diluted solutions, and high photochemical stability [12–15]. N,N′-bis (4-bromo-2,6-diisopropylphenyl)-1, 6, 7, 12-tetra [4-bromophenoxy] perylene-3, 4, 9, 10-tetracarboxylic diimide and N,N′-bis(4-bromo-2,6-diisopropylphenyl)-1, 6, 7, 12-tetra [4-Iodophenoxy] perylene-3, 4, 9, 10-tetracarboxylic diimide were used as the color-conversion layers for green and red emissions, respectively [12–15]. With the conventional lithography process, red and green color conversion layers (CCLs) were successfully deposited on blue LED.

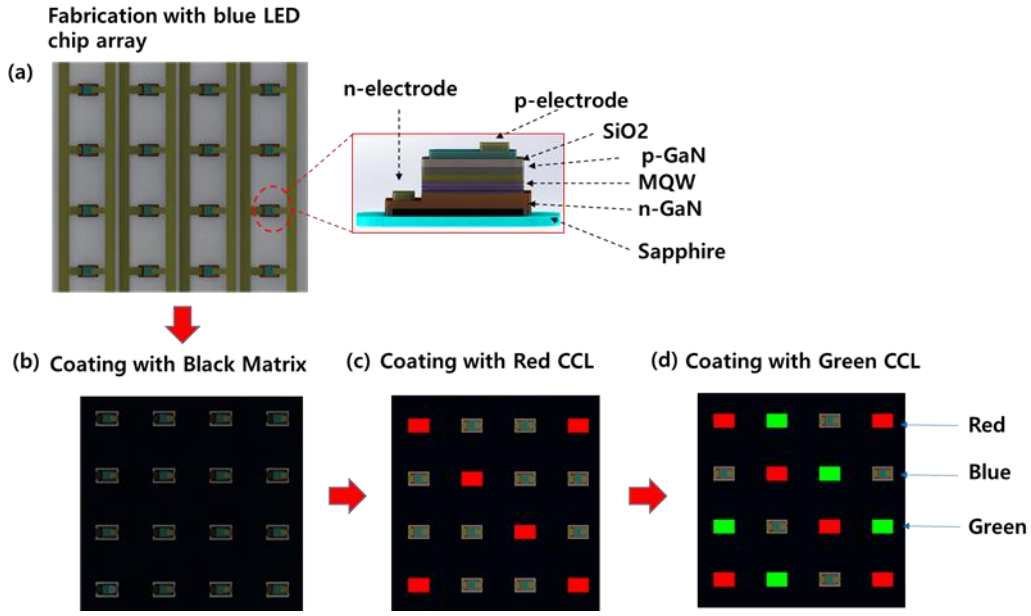

Figure 1. The schematic diagram of full-color micro LEDs based on photo-curable color-conversion materials.

3. Results and Discussion

Figure 2 details the transmittance of a 10 μm-thick photo-curable acrylic, where the thickness depends on the spin-coating rate of the photo-curable acrylic and the UV-visible absorption and photoluminescence (PL) spectroscopy for green and red dyes. Figure 2a,b indicates that the photo-curable acrylic had high transmittance in the visible range and the thickness could be increased by decreasing the spin-coating rate. For CCLs, we initially attempted to mix conventional phosphors such as β-SiAlON:Eu^{2+} and $CaAlSiN_3$:Eu^{2+} for green and red emissions. However, in terms of agglomeration of phosphor in acrylic, selectively patterning on blue LEDs was not possible, as shown by the Supplementary Figure S1a. This result was obtained due to the strong absorption of UV light by the aggregated phosphor particles.

Therefore, understanding the dispersion of color-conversion materials was important. We determined that nano-size organic materials were suitable for mixing with photo-curable acrylic, as shown in Supplementary Figure S1. With patterned CCLs, it is possible to fabricate full color arrays as shown in Supplementary Figure S2.

Before mixing the green and red nanosize dyes in photocurable acrylic, we tried to measure transmittance of the photocurable acrylic. The transmittance was almost 100% in the visible range. This result indicated that the photocurable acrylic could not absorb green and red light produced by color conversion. The thickness of acrylic materials could be increased by decreasing the spin coating rate. To confirm the possibility of color conversion of green and red dyes by blue light, we tried to measure the absorption and PL spectra using a 365 nm excitation. The result shows that blue light could be absorbed in green, and that green dyes and green and blue dyes emitted different peaks at 550 nm and 620 nm, respectively, as shown in Figure 2c,d. These results indicate that the blue and green dyes can be used as the color-conversion layer for full-color micro LEDs based on color-converted blue LED.

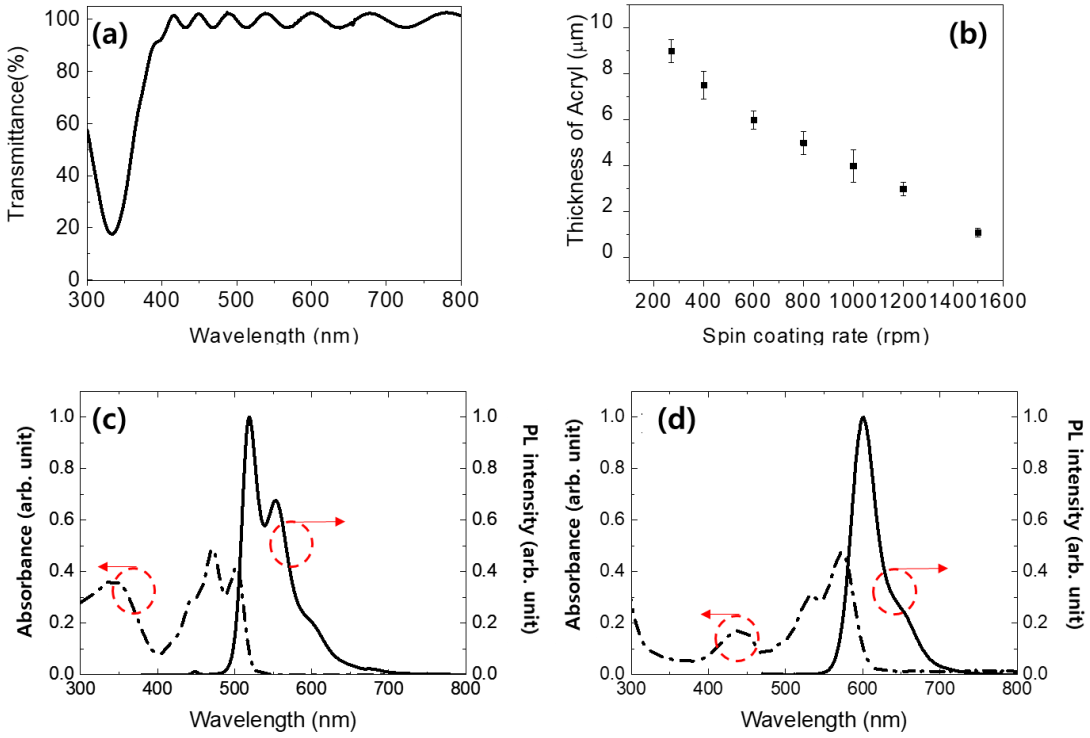

Figure 2. (**a**) Transmittance and (**b**) thickness of photocurable acrylic depending on spin coating rate, absorbance, and photoluminescence (PL) intensity of (**c**) green and (**d**) red dyes.

To identify the optimum conditions for CCL, we attempted to determine the optimum mixing ratios between photocurable acrylic and dye, and thickness.

To find the optimum mixing ratio between acrylic and dye, the conversion efficiency of blue to red or green light was measured as shown in Figure 3a,b. With increasing the mixing rate to 0.6 wt %, the conversion efficiency was improved by 47% and 35% for green and red dyes, respectively. However, when mixing rate was further increased, conversion efficiency was significantly decreased, owing to the aggregation of dye. The aggregation of dye can be attributed to the excimer formation and concentration induced quenching. [16] To find optimum thickness for color conversion, we tried to measure the PL spectra of green and red dyes, depending on the thickness of the mixture of photocurable acrylic and green/red dyes. Figure 3c,d shows the PL spectra of green and red dyes with the emission of blue LED. This spectrum shows that the blue leakage was decreased while green or red emission was increased with increasing thickness of the color-conversion layer. The full with half maximum (FWHM) of green and red dye was 78 nm and 52 nm, respectively. Figure 3e,f shows the normalized PL intensity of blue light and green or red light for the green and red dyes, respectively. When the thickness of CCLs is 3 μm, there was leakage of blue light as shown in Figure 3c,d. When increasing the thickness of the color-conversion layer, leakage of blue light was significantly decree sed and green or red emission was increased as shown in Figure 3e,f. We found that the color-conversion efficiency of red dyes was slightly lower than that of green dyes. This result can be attributed to low absorbance of the green dye of blue light compared to that of green dye. With deposition over the thickness of 7 μm, the leakage of blue light was significantly decreased. These results show it is possible to use a mixture of photocurable acrylic and green/red dye as the color-conversion layer for full-color micro LEDs if it is possible to deposit enough thickness of the color-conversion layer.

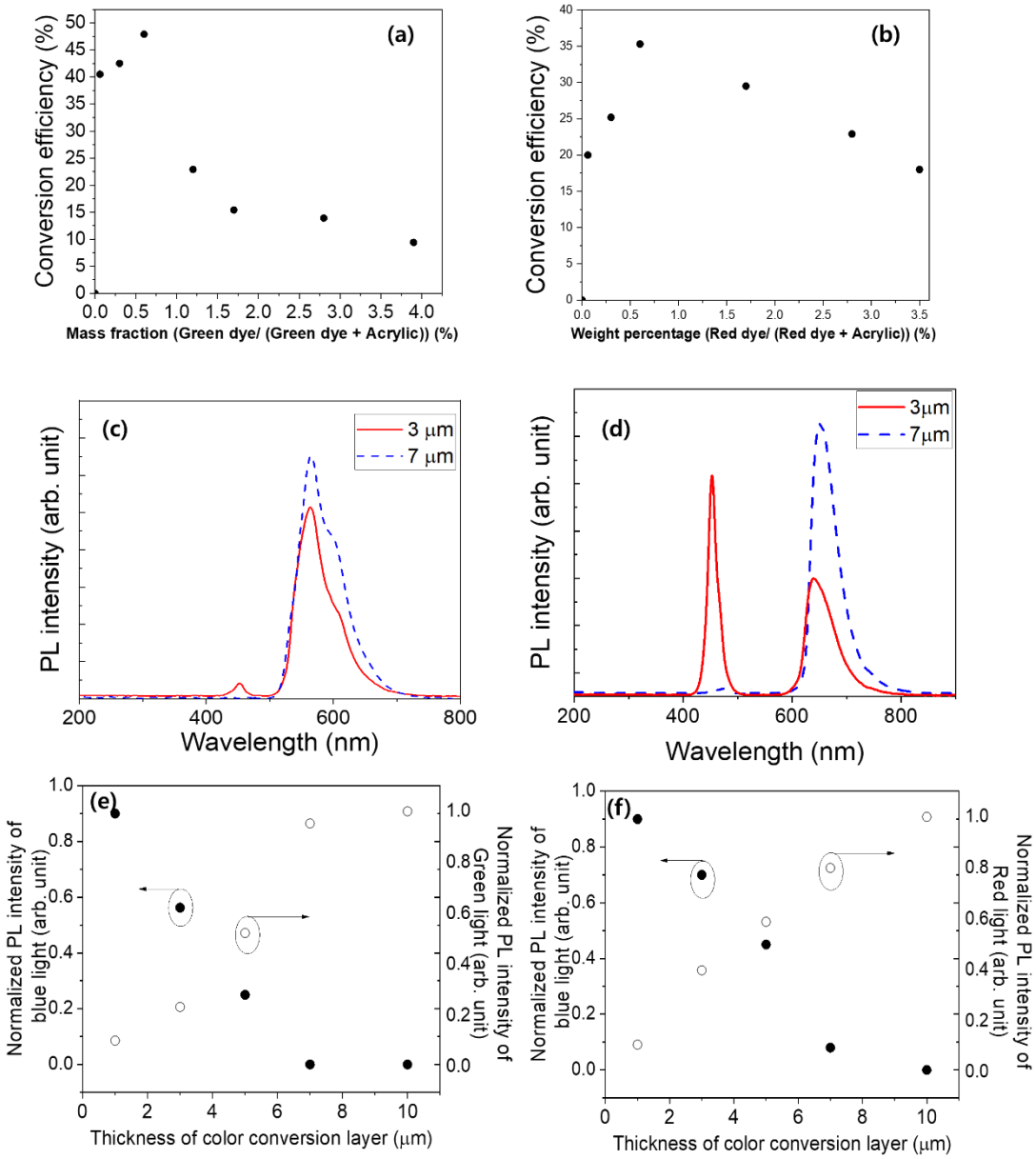

Figure 3. PL intensity of conversion efficiency of (**a**) green and (**b**) red dyes depending on mixing rate between acrylic and dye, and PL spectra of (**c**) green and (**d**) red dyes depending on thickness of color-conversion layer and normalized PL intensity of blue and green or red light of (**e**) green dyes and (**f**) red dyes.

Figure 4 presents the optical microscope image of the RGB array and its emission image, and the dependence of the electroluminescence (EL) spectra on the input current and color coordinate variations. As shown in Figure 4a, the red and green dyes were only selectively deposited on the blue LED. Figure 4b shows the emission image of full-color micro-LED arrays with an input current of 1 mA for each LED. The EL spectra of full-color micro LEDs are presented in Figure 4c. We found that the blue emission peak was slightly red-shifted. This can be resulted from the joule heating. In addition, with broadening of the spectrum of green and red dyes, there was overlapping of peaks. In addition, it is possible to induce unwanted light emission by absorption of the surrounding light. Although this method has many advantages, the efficiency of color conversion needs improvement. In addition, a visible light filter can be used to avoid absorption of the surrounding light. Approaches such as aggregation-induced emission are needed to improve the efficiency of color-conversion materials [17,18].

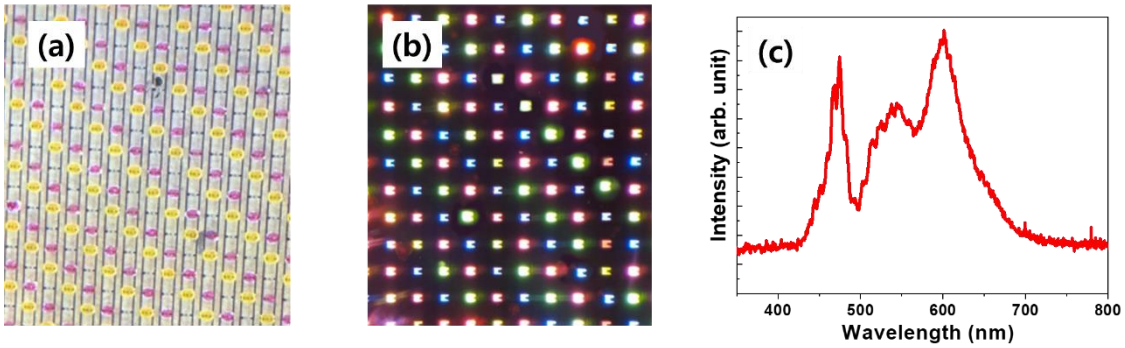

Figure 4. (**a**) Optical microscope image of full-color micro-LED arrays, (**b**) electroluminescence (EL) emission images, and (**c**) EL spectra.

4. Conclusions

We demonstrated the full-color LEDs using the conventional lithography technique based on a solution of acrylic resin and PAC, and green and red perylene bisimide dyes. With monolithic blue LEDs, it is possible to fabricate full-color RGB micro-LED arrays. It is simple to apply mass production in a controlled manner using the conventional lithography technique. This study provides a solution toward fabricating full-color micro-LED displays. Although this method has many advantages, the overall intensity and color-conversion efficiency are low, and the full-width of half maximum of red and green emissions is broad to use in a full-color display. However, we believe that these problems can be solved with improvement of the efficiency of the micro blue LED, with optimization of internal quantum efficiency, extraction efficiency, current spreading, and a decrease in heating, In addition, the color-conversion efficiency can be improved using the approaches of aggregation-induced emission and synthesis of high-efficiency fluorescent materials with a narrow emission spectrum.

Supplementary Materials: The following are available online at http://www.mdpi.com/2076-3417/10/6/2112/s1, Figure S1: Optical microscope images after lithography with (a) photocurable acrylic and β-SiAlON: Eu^{2+} and (b) photocurable acrylic and green dye. Figure S2: Schematic diagram of color-converted full-color R, G, B micro LEDs.

Author Contributions: W.H.K., Y.J.J., J.-Y.K., and M.-K.K. conceived and designed the experiments; W.H.K., M.K., K.Y., and M.H. performed the experiments; J.-Y.K., J.-H.R., and M.-K.K. analyzed data; and M.-K.K. wrote the paper. All authors have read and agreed to the published version of the manuscript.

Funding: This research was funded by LG display and the National Research Foundation (NRF) (NRF-2016R1D1A1B01013847 and 2018R1A2B6005352) funded by the Korea government.

Conflicts of Interest: The authors declare no conflict of interest.

References

1. Ding, K.; Avrutin, V.; Izyumskay, N.; Özgür, Ü.; Morkoç, H. Micro-LEDs, a Manufacturability Perspective. *Appl. Sci.* **2019**, *9*, 1206. [CrossRef]
2. Wu, T.; Sher, C.; Lin, Y.; Lee, C.; Liang, S.; Lu, Y.; Chen, S.; Guo, W.; Kuo, H.; Chen, Z. Mini-LED and Micro-LED: Promising Candidates for the Next Generation Display Technology. *Appl. Sci.* **2018**, *8*, 1557. [CrossRef]
3. Liu, Z.; Chong, W.C.; Wong, K.M.; Lau, K.M. GaN-based LED micro-displays for wearable applications. *Microelectron. Eng.* **2015**, *148*, 98–103. [CrossRef]
4. Huang, Y.; Tan, G.; Gou, F.; Li, M.; Lee, S.; Wu, S. Prospects and challenges of mini-LED and micro-LED displays. *J. Soc. Inf. Disp.* **2019**, *27*, 387–401. [CrossRef]
5. Gou, F.; Hsiang, E.L.; Tan, G.; Lan, Y.F.; Tsai, C.Y.; Wu, S.T. High performance color-converted micro-LED displays. *J. Soc. Inf. Disp.* **2019**, *27*, 199–206. [CrossRef]
6. Paranjpe, A.; Montgomery, J.; Lee, S.M.; Morath, C. Micro-LED displays: Key manufacturing challenges and solutions. *SID Int. Symp. Dig. Tech. Pap.* **2018**, *49*, 597–600. [CrossRef]

7. Chen, S.H.; Shen, C.; Wu, T.; Liao, Z.; Chen, L.; Zhou, J.; Lee, C.; Lin, C.; Lin, C.; Sher, C.; et al. Full-color monolithic hybrid quantum dot nanoring micro light-emitting diodes with improved efficiency using atomic layer deposition and nonradiative resonant energy transfer. *Photonics Res.* **2019**, *7*, 416–422. [CrossRef]
8. Kang, C.; Lee, J.; Kong, D.; Shim, J.; Kim, S.; Mun, S.; Choi, S.; Park, M.; Kim, J.; Lee, D. Hybrid full-color inorganic light-emitting diodes integrated on a single wafer using selective area growth and adhesive bonding. *ACS Photonics* **2018**, *5*, 4413–4422. [CrossRef]
9. Han, H.; Lin, H.; Lin, C.; Chong, W.; Li, J.; Chen, K.; Yu, P.; Chen, T.; Chen, H.; Lau, K.; et al. Resonant-enhanced full color emission of quantum-dot-based micro-LED display technology. *Opt. Express* **2015**, *23*, 32504–32515. [CrossRef] [PubMed]
10. Lin, H.; Sher, C.; Hsieh, D.; Chen, X.; Chen, H.P.; Chen, T.; Lau, K.; Chen, C.; Lin, C.; Kuo, H. Optical cross-talk reduction in a quantum-dot-based full-color micro-light-emitting-diode display by a lithographic-fabricated photoresist mold. *Photonics Res.* **2017**, *5*, 411–416. [CrossRef]
11. Chen, G.; Wei, B.; Lee, C.; Lee, H. Monolithic red/green/blue micro-LEDs with HBR and DBR structures. *IEEE Photonics Technol. Lett.* **2018**, *30*, 262–265. [CrossRef]
12. Huang, C.; Barlow, S.; Marder, S.R. Perylene-3,4,9,10-tetracarboxylic Acid Diimides: Synthesis, Physical Properties, and Use in Organic Electronics. *J. Org. Chem.* **2011**, *76*, 2386–2407. [CrossRef] [PubMed]
13. Hariharan, P.S.; Pitchaimani, J.; Madhu, W.; Anthony, S.P. Perylene Diimide Based Fluorescent Dyes for Selective Sensing of Nitroaromatic Compounds: Selective Sensing in Aqueous Medium Across Wide pH Range. *J. Fluoresc.* **2016**, *26*, 395–401. [CrossRef] [PubMed]
14. Zhang, L.; He, D.; Kun, Y.L.; Guo, W.Z.; Lin, J.; Zhang, H. 2,5,8,11-Tetraalkenyl Perylene Bisimides: Direct Regioselective Synthesis and Enhanced π–π Stacking Interaction. *Org. Lett.* **2016**, *18*, 5908–5911. [CrossRef] [PubMed]
15. Lee, S.M.; Jeong, Y.T. Synthesis and Characterization of red organic fluorescent of perylene bisimide derivations. *J. Korean Inst. Electr. Electron. Mater. Eng.* **2017**, *30*, 577–582.
16. Fennel, F.; Gershberg, J.; Stolte, M.; Würthner, F. Fluorescence quantum yields of dye aggregates:a showcase example based on self-assembled perylene bisimide dimers. *Phys. Chem. Chem. Phys.* **2018**, *20*, 7612–7620. [CrossRef] [PubMed]
17. Ananthakrishnan, S.J.; Varathan, E.; Ravindran, E.; Somanathan, N.; Subramanian, V.; Mandal, A.B.; Sudhacd, J.D.; Ramakrishnanc, R. A solution processable fluorene–fluorenone oligomer with aggregation induced emission enhancement. *Chem. Commun.* **2013**, *49*, 10742–10744. [CrossRef] [PubMed]
18. Luo, J.; Xie, Z.; Lam, J.W.Y.; Cheng, L.; Chen, H.; Qiu, C.; Kwok, H.S.; Zhan, X.; Liu, Y.; Zhu, D.; et al. Aggregation-induced emission of 1-methyl-1,2,3,4,5-pentaphenylsilole. *Chem. Commun.* **2001**, 1740–1741. [CrossRef] [PubMed]